

How do high-latitude North Atlantic climate signals the crossover between the Deep Western Boundary Current and the Gulf Stream?

Jiayan Yang

Department of Physical Oceanography, Woods Hole Oceanographic Inst., Woods Hole, Massachusetts, USA

Terrence M. Joyce

Department of Physical Oceanography, Woods Hole Oceanographic Inst., Woods Hole, Massachusetts, USA

Received 22 April 2002; accepted 6 September 2002; published 25 January 2003.

[1] A simple model is used to examine how the presence of a continental slope along the western boundary, and wind-driven gyres, especially the Gulf Stream (GS) jet, affect the pathways of water-mass flow and wave propagation in the abyssal ocean. Two types of forcing: an interior source and a boundary inflow (to mimic the Labrador Sea Water and the marginal-sea overflow), are considered here. Both topography and wind-driven gyres considerably alter how the water mass spreads from the source (in the steady state case) and how transient signals propagate to the unforced regions. Sloping bathymetry near the western boundary allows for meridional propagation of topographic waves. The GS jet creates a strong meridional PV gradient which could partially block the southward water-mass transport and wave propagation. The effectiveness of the crossover to disrupt the lower layer response depends on the type of high latitude water mass forcing. *INDEX TERMS*: 1620 Global Change: Climate dynamics (3309); 4219 Oceanography: General: Continental shelf processes; 4532 Oceanography: Physical: General circulation. **Citation**: Yang, J., and T. M. Joyce, How do high-latitude North Atlantic climate signals the crossover between the Deep Western Boundary Current and the Gulf Stream?, *Geophys. Res. Lett.*, 30(2), 1070, doi:10.1029/2002GL015366, 2003.

1. Introduction

[2] Changes in high latitude production of the various components of North Atlantic Deep Water (NADW) are of considerable interest as they have been linked to changes in global climate state. The mechanism of teleconnection between changes in the high latitude N. Atlantic and the global atmosphere are not clear, however. Various arguments have been made that global climate change may not be sensitive to high latitude N. Atlantic variability via the atmospheric pathway and there is some growing interest in the role of the tropical Pacific Ocean in the problem of global climate change [Cane, 1998]. Recently Huang *et al.* [2000] have argued that the ocean may provide the teleconnection bridge by rapidly exporting atmospheric signals that affect the N. Atlantic Ocean through internal Kelvin and Rossby wave propagation. These can spread information about rapid change in the thermocline depth globally.

[3] We wish to investigate other aspects of ocean dynamics that might affect the southward transmission of signals

arising from high latitude changes in NADW production. These deal with the effects upon the deep water wave guide (a path along which waves propagate) due to changes in the thermocline depth associated with sloping topography and the wind-driven circulation, with special emphasis on the region where the Deep Western Boundary Current (DWBC) crosses under the surface Gulf Stream near Cape Hatteras. This modeling study follows in the spirit of a kinematic model by Hogg and Stommel [1985], and observational results by Pickart and Smethie [1993] and Bower and Hunt [2000] showing that the time mean or synoptic DWBC path could be substantially affected by the overlying Gulf Stream. It is also offered to explain why signals of change in the thickness of Labrador Sea Water (LSW), one of the least dense flavors of NADW, can be detected at Bermuda 6 years later [Curry *et al.*, 1998], even though Bermuda is not located along the western boundary, where signals of rapid change are expected to propagate. Our model is much simpler than one in which Spall [1996] examined the interaction of the two currents at the crossover point. In that study, the separated Gulf Stream created a rich field of eddies, developed recirculation pathways and interacted with the NADW layer via changes in the recirculation gyres. Time variability developed due to changes in the baroclinic stability of the system in the region of the crossover point. Because the DWBC in this region is found at and above the continental slope, both the existence of a sloping boundary and the depth change across the Gulf Stream are important elements of the dynamics for all of these studies.

[4] Our study will combine aspects of the above investigations by including time dependence, but not eddies, with the dynamics of the crossover. We will do this by including the effects of sloping topography and an upper layer thermocline depth structure due to the Gulf Stream on the dynamics of the lower layer, ignoring any upper ocean physics other than what is needed to produce the sloping thermocline. In the next section, we will present the model for the lower, time-dependent layer. This will be followed by an examination of time-dependent studies resulting from two different methods for changing the source of the anomalous deepwater production: internal forcing away from lateral boundaries (to mimic changes in LSW production) and injection of fluid at the northern boundary (to mimic effects of changes in the Greenland-Iceland-Norwegian (GIN) Sea overflow) into the basin. Steady state solutions are then presented and results are briefly discussed in the final section.

2. Model Description

[5] We use a 1.5 layer and linear reduced gravity model. The GS and wind-driven gyres in the upper layer are specified in each case and will be discussed later. It is assumed that the effect of wind-stress forcing is limited in the upper layer only, and the lower layer is forced by sources/sinks of water masses. Our interest is in the deep ocean layer which is governed by the following equations:

$$\frac{\partial u}{\partial t} - fv + g' \frac{\partial h}{\partial x} = A_H \nabla^2 u \quad (1)$$

$$\frac{\partial v}{\partial t} - fu + g' \frac{\partial h}{\partial y} = A_H \nabla^2 v \quad (2)$$

$$\frac{\partial h}{\partial t} + \frac{\partial(Hu)}{\partial x} + \frac{\partial(Hv)}{\partial y} = S(x,y) \quad (3)$$

where $\vec{u} = (u,v)$ is the velocity, h and $H(x,y)$ are anomalous and mean layer thickness respectively, $A_H = 10^3 \text{ m}^2\text{s}^{-1}$ is the lateral viscosity, $g' = 0.0032 \text{ ms}^{-2}$ is a reduced gravity (which yields a Kelvin wave speed of about 2.2 m/s in the deep basin of 1500 m, approximately for the first baroclinic mode), and $S(x,y)$ is a prescribed source of mass volume to be discussed below. The β -plane (centered at 35°N) is used here. The northern and western boundaries are closed and no-slip and no-normal flow conditions are applied along them. The eastern and southern boundaries are open where we use a simple open boundary condition: $\partial(u,v,h)/\partial n = 0$ (where n is the length vector perpendicular to the open boundary).

[6] The mean layer thickness $H(x,y)$ varies spatially according to bottom topography and the thermocline depth in the upper layer. In the first case, it is assumed that thermocline depth is flat so that H is affected only by the presence of a continental slope along the western boundary. The slope is chosen so that H increases linearly from 500 meters at $x = 0$ to 1200 meters at $x = 800 \text{ km}$ (Figure 1a). The corresponding field of potential vorticity (PV), f/H , is shown in the right column of Figure 1a. The next two versions of model geometry use the same bottom topography, but also include thermocline-depth variations. In the second case, a zonal jet is specified in the upper layer to represent the Gulf Stream after its separation from the western boundary. The thermocline depth is adjusted according to geostrophy. The resulting $H(x,y)$ and its associated PV field are shown in Figure 1b. In the last case, we consider both the Gulf Stream jet and the two wind-driven gyres (Figure 1c). The wind stress is chosen to be zonally uniform and to vary sinusoidally in the meridional direction. The thermocline depth in the interior is solved analytically according to the Sverdrup relation in a 1.5 layer model and then matched to the western boundary layer solution. We will focus most our discussion on the last case with double gyres (Figure 1c). The first two cases of $H(x,y)$ (Figures 1a–1b) are extreme and are used only to illustrate the effects of topography and GS jet so that the results from the more realistic case can be better elucidated.

[7] In all experiments to be presented, the model is driven by a single water-mass source. In the LSW-type forcing, it enters through $S(x,y)$ in equation (3) and is distributed as a

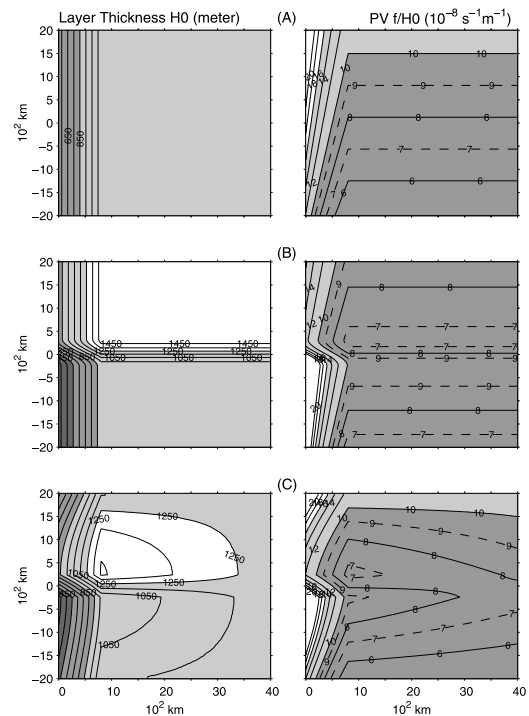


Figure 1. Model geometry is shown for three different scenarios. In all cases the lower layer depth ($H(x,y)$) is shown on the left panels, while lower layer PV ($=f/H$) is on the right. In the first case, only a continental slope is present at the western boundary; total depth change across the linear bottom slope is 700 m (from 500 m to 1200 m). In the second case, a zonal upper layer jet emerges from the western boundary to simulate the crossover. The bottom layer thickness reflects the altered topography due to the bottom slope and the zonal jet, which has a depth change of 500 m across the GS jet. In the third case, the zonal jet decays linearly with longitude as two gyres redistribute the interior flow.

Gaussian function in an area between $x = 1000$ and 1500 km and $y = 1000$ and 1500 km . In the GIN-Sea outflow cases, an inflow along the northern boundary is specified at the northeastern corner.

3. Time Dependent Results

[8] In what follows the water-mass source was set to oscillate from -1 to $+1 \text{ Sv}$ with an 8-year period. This is meant to simulate response to interannual variation of the water-mass source. The waves in the system are fairly non-dispersive, so these runs are applicable to other periods of forcing. Since the model is linear, the magnitude of the model variables (such as h) is proportional to the strength of the forcing term.

[9] First we consider a LSW-type source, located in the NW part of the ‘subpolar’ gyre, near the sloping topography at the western boundary. This will be followed by a GIN overflow simulation, again with an 8 year period of forcing. Because of space limitations, we will concentrate only on the double gyre case (with $H(x,y)$ shown in Figure 1c). In this case, the DWBC encounters an eastward jet and sloping topography near $y = 0$, but this jet feeds into both gyres with a linearly decreasing transport as it moves eastward. Two

recirculating ‘gyres’ are found on both sides of the separated jet and their interior depth structure provide pathways of closed f/H for waves to propagate in the lower layer.

[10] For the LSW case, we show (Figure 2, left panels) anomalous lower layer thickness at times of 2, 4, 6 and 8 years. The pathways for wave propagation are guided by the f/H topography and the initial latitude and location of the source in Figure 1c. Initially, the signal propagates westward as a normal Rossby wave but encounters the sloping topography and refracts southward along the f/H slope, reaching the crossover point at about 4 years as a topographic Rossby wave (TRW; the term ‘topographic’ here can be due to either the bottom slope or the thickness variation in the upper layer). The signal then could bifurcate, part continuing along the western slope to the south and part moving eastward under the surface Gulf Stream as an eastward propagating topographic wave (due to the thickness change in the upper layer). However, in the run presented, the TRW has not propagated far enough to the west up the slope and thus all signals are deflected offshore at the crossover. By the time the signal has reached this crossover point, the source has begun to change to a negative thickness anomaly and this negative anomaly propagates southward in a similar manner as its positive counterpart. Note that there are no internal Kelvin waves along the western boundary because the initial Rossby wave never reached the vertical wall at the west within the domain. Under the jet, the signal propagates offshore and then returns to the slope where it slowly moves closer to the boundary again in its southward TRW pathway. We see that an observer at Bermuda in the model (south of the jet, within the westward recirculation regime (near $x = 1000$ km, $y = -500$ km) is within the waveguide. In the model it takes about 5 years to reach this point, although this is not meant to be a realistic simulation of the ocean and such close agreement should not be expected. However, this signal gets there without any mean flow in the lower layer!

[11] The wave propagation is considerably different in the two extreme $H(x,y)$ cases. In the topography-alone case (Figure 1a), incoming long Rossby waves refract into topographic Rossby waves and propagate southwestward along the f/H contours (not shown). There is no GS jet to cross under in this case. In the case with a GS jet (Figure 1b), the PV contour line of $9 \times 10^{-8} \text{ m}^{-1}\text{s}^{-1}$ (dashed line in the right panel of Figure 1b) blocks the wave signals from crossover with the GS jet. Consequently, all wave energy propagates offshore at the crossover point (not shown), and time dependent signals are completely blocked from the ‘subtropical’ gyre.

[12] For the double gyre case with a GIN forcing (Figure 2, right panels), a source in the NE corner has propagated across the entire domain by 2 years as an internal Kelvin wave, and one can begin to see scattering into topographic energy over the slope at both the NW corner and at the crossover point. This signal continues to move southward from each of these points along the slope as a TRW until the northern signal is diverted to the east under the Gulf Stream, although much less than the previous case. This is because the signal is close enough to the wall to follow f/H lines that pass through the jet with some deflection. At 4 years the TRW has reached the southern boundary, 2 years ahead of the LSW case. As we can see from both types of sources,

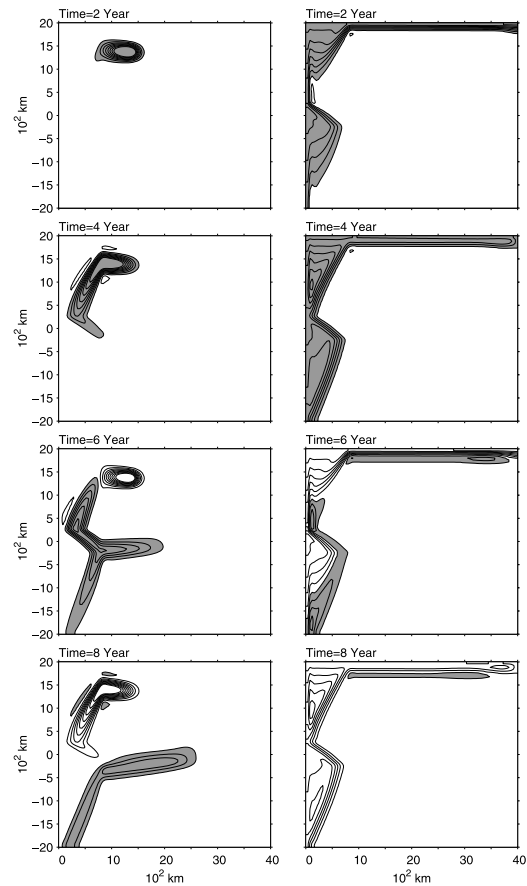


Figure 2. For model 3 (Figure 1, lower panels), four 2 year snapshots spanning one complete cycle of lower layer thickness anomaly are shown for an oscillating source of the LSW type (left panels) or GIN type (right panels). The contour interval is 25 m and 5 m for the left and right panels respectively.

most of the variability gets through the crossover point into the subtropical gyre, and the GIN simulation shows less effect of the jet upon the waveguide. The result in the topography-alone case (not shown) is similar except that no TRW was formed near $y = 0$ since there is no GS jet. With a strong GS jet case some wave energy is refracted off shore (not shown).

[13] It is interesting to note that the amplitude of h for the LSW-type forcing is considerably greater than that in the GIN forcing (contour interval is 25 m for the left panels and 5 m for the right panels). This is mostly due to the presence of Kelvin waves in the latter case which rapidly export the mass anomaly through the southern boundary.

4. Steady-State Result

[14] The model was run to steady state after a step function source strength of 1 Sv was imposed from an initial state of rest. Because the southern and eastern boundaries are open in all of the results presented here, there is no interior adjustment due to Kelvin waves on the eastern or southern boundary and Rossby wave radiation from the eastern boundary. For the LSW case (Figure 3, left panels), an anticyclonic circulation develops around a thicker lower

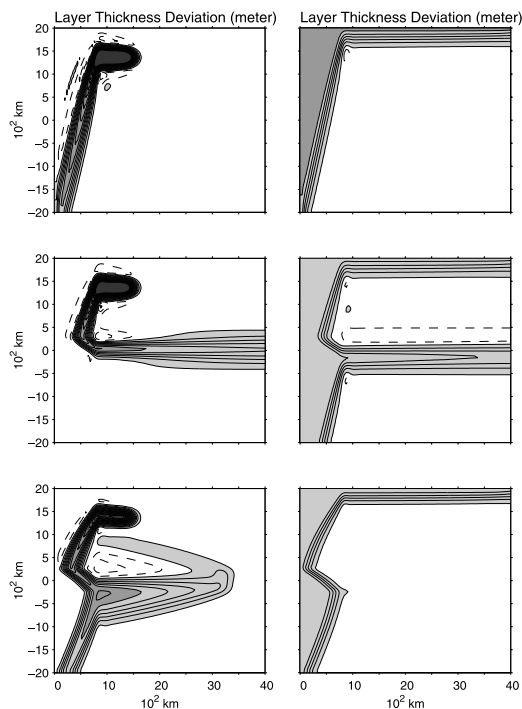


Figure 3. For each of the three models in Figure 1, we show the steady state response to an increase in thickness of the lower layer due to an addition of mass in the ‘interior’ (LSW case, left panels) or entering the domain at the NE corner (GIN case, right panels). In all runs, the southern and eastern boundaries are open so that no interior spin up has occurred by Kelvin and/or Rossby wave propagation except along the northern and western boundaries. The LSW cases are examples of beta-plumes modified by topographic Rossby wave dynamics. Lower layer mean flows are anticyclonic around the positive height anomaly. In the GIN case a net southward transport is set up along the western boundary by a combination of Kelvin and TRW dynamics. Areas of positive h are shaded. The contour interval is 20 m for the left panel (LSW cases) and 10 m for the right panel (GIN cases).

layer. This structure is highly distorted by the fH topography. In the GIN case, the flow is unidirectional except for the zonal jet simulation where a deep eastward flow is found under the jet and a westward flow to its south (Figure 3, right panels). Note that for both types of sources, there is a net transport of water out of the basin. This is accomplished in the LSW case by the fact that thickness of the equatorward flow is greater than that of the poleward flow producing a net equatorward transport even though there is a flow reversal. Mean recirculation gyres develop to varying degree. The most notable difference in the extent of the recirculation gyres is case 3, in which the topography of the thermocline reflects a pair of counter-rotating gyres in the upper layer. In this case, the LSW source develops a pair of co-rotating recirculating gyres in the lower layer on either side of the upper layer jet, while the GIN source shows a DWBC which moves offshore under the jet but continues southward with no deep recirculation. While shifts of the LSW source influence the details of the mean flow, in general, the LSW simulations show much more disruption from the ‘slope

topography only’ geometry and sensitivity to the upper layer depth structure that the GIN simulations, as could be anticipated from the preceding time dependent results.

5. Discussion

[15] Our study examines how the GS and topography affect the pathways of two different types of water masses: one is formed in the interior ocean and the other is supplied from an inflow. The sensitivity to the crossover is very different for these two different types of water masses, for both steady and transient cases. The effectiveness of the crossover on the trapping and/or shifting of the waveguide for each type of water mass sources depends on the GS strength, the gyre circulation, and topography. A stronger wind-stress forcing in the upper layer will increase the barrier effect of GS on the southward transport of deep water and propagation of wave signals. Our sensitivity tests (not shown) showed that a very strong GS jet could completely block the waves induced by the LSW-type of forcing, thus blocking signals such as observed by *Molinari et al.* [1998] from extending south of the crossover point. If the wind-driven gyres and particularly the GS jet vary with time, it is likely that temporal climate variations can be induced in the lower layer even if the forcing in that layer is steady. The existence of a second crossover point near the SE corner of the Grand Banks could provide another site where LSW anomalies could get diverted [Lavender et al., 2000] to the east rather than continuing southward along the western boundary.

[16] **Acknowledgments.** This study has been supported by the NOAA CLIVAR-Atlantic Program (grant numbers: NA96GP0464 and NA16GP1573) and by NASA Physical Oceanography Program (contract number: 1217578). We thank Drs. A. Bower, M. Spall, R. Pickart and J. Toole for their comments. WHOI contribution number 10822.

References

- Bower, A. S., and H. D. Hunt, Lagrangian Observations of the Deep Western Boundary Current in the North Atlantic Ocean, part II: The Gulf Stream-Deep Western Boundary Current Crossover, *J. Phys. Oceanogr.*, **30**, 784–804, 2000.
- Cane, M. A., A role for the tropical Pacific, *Science*, **282**, 59–61, 1998.
- Curry, R. G., M. S. McCartney, and T. M. Joyce, Oceanic transport of subpolar signals to mid-depth subtropical waters, *Nature*, **391**, 575–577, 1998.
- Hogg, N. G., and H. Stommel, On the relation between the deep circulation and the Gulf Stream, *Deep-Sea Res.*, **32**, 1181–1193, 1985.
- Huang, R. X., M. A. Cane, N. Naik, and P. Goodman, Global adjustment of the thermocline in response to deepwater formation, *Geophys. Res. Lett.*, **27**, 759–762, 2000.
- Lavender, K. L., R. E. Davis, and W. B. Owens, Mid-depth recirculation observed in the interior Labrador and Irminger Seas by direct velocity measurements, *Nature*, **407**, 66–69, 2000.
- Molinari, R. L., R. A. Fine, W. D. Wilson, R. Curry, J. Abell, and M. S. McCartney, The arrival of recently formed Labrador Sea Water in the Deep Western Boundary Current at 26.5°N, *Geophys. Res. Lett.*, **25**, 2249–2252, 1998.
- Pickart, R. S., and W. M. Smethie Jr., How does the Deep Western Boundary Current cross the Gulf Stream?, *J. Phys. Oceanogr.*, **23**, 2602–2616, 1993.
- Spall, M. A., Dynamics of the Gulf Stream/Deep Western Boundary Current crossover, part I: Entrainment and recirculation, *J. Phys. Oceanogr.*, **26**, 2152–2168, 1996.